

# 2D Nanomaterial, $Ti_3C_2$ MXene-Based Sensor to Guide Lung Cancer Therapy and Management †

Mahek Sadiq <sup>1</sup>, Lizhi Pang <sup>2</sup>, Michael Johnson <sup>3</sup>, Venkatachalem Sathish <sup>2</sup>  
and Danling Wang <sup>1,3,4,\*</sup>

<sup>1</sup> Biomedical Engineering Program, North Dakota State University, Fargo, ND 58108, USA; mahek.sadiq@ndsu.edu

<sup>2</sup> Department of Pharmaceutical Science, North Dakota State University, Fargo, ND 58108, USA; lizhi.pang@ndsu.edu (L.P.); s.venkatachalem@ndsu.edu (V.S.)

<sup>3</sup> Materials and Nanotechnology Program, North Dakota State University, Fargo, ND 58108, USA; michael.johnson.1@ndsu.edu

<sup>4</sup> Department of Electrical and Computer Engineering, North Dakota State University, Fargo, ND 58108, USA

\* Correspondence: danling.wang@ndsu.edu; Tel.: +1-701-231-8396

† Presented at the 1st International Electronic Conference on Biosensors, 2–17 November 2020; Available online: <https://iecb2020.sciforum.net/>.

Published: 2 November 2020

**Abstract:** Major advances in cancer control can be greatly aided by early diagnosis and effective treatment in its pre-invasive state. Lung cancer (small cell and non-small cell) is a leading cause of cancer-related death among both men and women around the world. A lot of research attention has been attracted to diagnosing and treating lung cancer. A common method of lung cancer treatment is based on COX-2 (Cyclooxygenase-2) inhibitors. This is because COX-2 is commonly over expressed in lung cancer and also the abundance of its enzymatic product Prostaglandin E<sub>2</sub> (PGE<sub>2</sub>). Instead of using traditional COX-2 inhibitors to treat lung cancer, here, we report a new anti-cancer strategy recently developed for lung cancer treatment. It adopts more abundant omega-6 ( $\omega$ -6) fatty acids such as dihomo- $\gamma$ -linolenic acid (DGLA) in the daily diet and the commonly high levels of COX expressed in lung cancer to promote the formation of 8-hydroxyoctanoic acid (8-HOA) through a new delta-5-desaturase (D5Di) inhibitor. The D5Di will not only limit the metabolic product, PGE<sub>2</sub> but also promote the COX-2 catalyzed DGLA peroxidation to form 8-HOA, a novel anti-cancer free radical byproduct. Therefore, the measurement of the PGE<sub>2</sub> and 8-HOA levels in cancer cells can be an effective method to treat lung cancer by providing in-time guidance. A novel sensor based on a newly developed functionalized nanomaterial, 2-dimensional nanosheets,  $Ti_3C_2$  MXene, has proved to sensitively, selectively, precisely and effectively detect PGE<sub>2</sub> and 8-HOA in A549 lung cancer cells. Due to the multilayered structure and extremely large surface area, metallic conductivity and easy and versatile in surface modification,  $Ti_3C_2$  MXene-based sensor will be able to selectively adsorb different molecules through physical adsorption or electrostatic attraction, and lead to a measurable change in the conductivity of the material with high signal-to-noise ratio and excellent sensitivity.

**Keywords:** 2D  $Ti_3C_2$  MXene; PGE<sub>2</sub>; 8-HOA; lung cancer

---

## 1. Introduction

The most common cancers occur in lungs, breast, pancreas, colon, skin and stomach [1]. Lung cancer is the second most common cancer in men and women and the first leading cause of cancer deaths in the United States. The two major types of lung cancer are: small cell lung cancer (SCLC, ~15%) [2] and non-small cell lung cancer (NSCLC, ~85%) [3]. The survival rate of both types of lung

cancer is very low [4]. According to the American Cancer Society, lung cancer and asbestos-related lung cancer [5] alone are responsible for 142,670 estimated deaths in 2019, making it the number one killer and three times deadlier than breast cancer [6]. This is because most patients (~75%) have been diagnosed at a late stage of the disease (stage III or IV) [7]. To increase the survival rate, major advances in lung cancer control or prevention will be greatly aided by early detection and effective anti-cancer therapy. In recent years, a variety of therapeutic and adjuvant methods and nutritional approaches have been developed for lung cancer treatment such as chemotherapy, targeted therapy [8,9], cyclooxygenase (COX)-2 inhibition [10], and omega-3 fatty acid dietary manipulation [11,12].

Besides these methods, many physical 'visualization/detection' methods [13] are available for tumor detection and cancer diagnosis [14]. Some of them are Positron Emission Tomography (PET), Magnetic Resonance Imaging (MRI), Computerized Tomography (CT), Ultrasonography, Endoscopy and Gas Chromatography method. However, these methods have some major issues for applications in cancer diagnosis. For example, MRI is very expensive and time-consuming. Sometimes it even cannot distinguish between malignant and benign cancer [15]. In case of PET, radioactive material is used which is combined with glucose and injected into the patient. This might be a health concern for diabetic patients [16]. High-dose radiation involved in CT scanning can even increase the risk of cancer [17]. Ultrasound, however, cannot provide accurate diagnosis and frequently has trouble to determine whether a mass is malignant or not [18]. Endoscopy is relatively safer but still has complications like perforation, infection, bleeding and pancreatitis [19]. The fundamental limitation of gas chromatography is that the substance must be volatile. It means that a finite portion of the substance needs to be distributed into the gaseous state [20]. It is problematic to use Gas Chromatography Mass Spectroscopy (GC-MS) in cancer detection because its sampling procedure is very complicated and the results are difficult to interpret. This technique is very expensive and must be operated by a very skilled personnel [21]. Therefore, an effective and accurate technique to detect tumor and diagnose cancer is urgently needed.

In particular, studies have confirmed that cyclooxygenase (COX), typically the inducible form COX-2, is commonly over expressed in lung cancer and the abundance of its enzymatic product prostaglandin E<sub>2</sub> (PGE<sub>2</sub>) plays an important role in influencing cancer development. Since PGE<sub>2</sub> is a deleterious metabolite formed from COX-2-catalyzed peroxidation of an upstream omega-6 ( $\omega$ -6) fatty acid called arachidonic acid (AA), PGE<sub>2</sub> promotes tumor growth and metastasis [22]. So, it can be taken as an indicator of local COX activity to regulate or control lung cancer. Many efforts on treating lung cancer have been focused on the development of COX-2 inhibitors because they can be used to suppress prostaglandin E<sub>2</sub> (PGE<sub>2</sub>) formation from COX-2-catalyzed  $\omega$ -6 arachidonic acid peroxidation [23]. However, most COX-2 inhibitors can severely injure the gastrointestinal tract, increase the risk of cardiovascular disease, and provide limited clinical responses [22,23]. To seek a safer and more efficient method to treat cancers, a new anti-cancer strategy [24], as shown in Figure 1, has been recently developed which is a very different approach than the classic COX-2 inhibitors [24–26]. In detail, this is a strategy which adopts more abundant  $\omega$ -6s such as dihomo- $\gamma$ -linolenic acid (DGLA) in the daily diet and the commonly high level of COX expressed in most cancers to promote the formation of 8-hydroxyoctanoic acid (8-HOA) through using a newly developed inhibitor, delta-5-desaturase (D5Di) inhibitor. This is because the D5Di is an enzyme that converts an upstream DGLA in diet to AA. The high expression of COX-2 will promote the conversion of AA to PGE<sub>2</sub>, while the D5Di will 1) knock down the conversion of DGLA to AA and limit the metabolic product, PGE<sub>2</sub>; 2) promote the COX-2 catalyzed DGLA peroxidation to form 8-HOA, a novel anti-cancer free radical by-product. This strategy has proven to produce more effective and safer therapeutic outcomes in cancer treatment and be validated in the colon and pancreatic cancers [27]. Therefore, detection of the PGE<sub>2</sub> and 8-HOA in lung cancer should be an effective method to evaluate the efficiency of the cancer treatment. Furthermore, the relative ratio of PGE<sub>2</sub> and 8-HOA concentrations can become a useful adjuvant method to help diagnose cancers at an early stage. Therefore, it is very critical to develop a technique or device, which can track PGE<sub>2</sub> and 8-HOA concentrations in cancer and provide in-time guidance and feedback for cancer treatment and prevention. However, due to the extremely low concentrations of PGE<sub>2</sub> and 8-HOA in cancer cells ~ ng/mL or  $\mu$ M, the detection of

these components is quite challenging. The traditional methods to measure low concentration of compounds, such as PGE<sub>2</sub> and 8-HOA, are using gas chromatography-mass spectrometry (GC-MS) or liquid chromatography-mass spectrometry (LC-MS). These techniques, as described above, are accurate and sensitive but heavy (not portable), expensive (skilled personnel to operate) and time-consuming. Recent advances in nanofabrication technology have made it possible to be widely used in electronics, sensing, biomaterials for variable areas including disease diagnosis and control in medicine, drug delivery, and food industry [28–31]. Due to the increased surface areas and the feasibility of controllable size and surface properties, nanomaterials such as nanofibers, nanowires, nanoparticles provide great opportunities for the development of advanced sensing systems and portable device/instrumentation with improved sensitivity, and selectivity [32–38]. In particular, the use of structure-directing synthetic approaches in nanomaterial synthesis allows the preparation of particularly promising nanomaterials by tailoring nanomaterial crystalline phase, surface states, morphology, and facets for specific sensing application. With the development of two-dimensional (2D) nanomaterials such as graphene, these type of materials have gained tremendous attention because of their astonishing electrical and optical properties featured with “all-surface” nature [39–43]. Such all-surface nature can offer great opportunities to tailor material properties through surface treatment for targetable detection. In 2011, the birth of MXenes introduced a new family into the two-dimensional (2D) materials and further proves to be promising in the flexible sensory application due to its controllable preparation method and fascinating properties. In essence, MXenes consists of transition metals (including Ti, V, Nb, Mo, etc.) and carbon or nitrogen, sharing a general formula of  $M_{n+1}X_n$  ( $n = 1-9$ ). As a new star of 2D materials, MXenes have the metallic conductivity and hydrophilic nature due to their uncommon surface terminations. The unique accordion-like morphology (Figure 2), excellent conductivity, and rich but tailorable surface functional groups endow MXenes with attractive electronic, mechanical, physical and chemical properties for applications in energy storage [44], environmental science [45] and sensors [46]. In this paper, we report a new sensor based on a newly developed 2-dimensional nanomaterial, Ti<sub>3</sub>C<sub>2</sub> MXene. The preliminary data indicate that this device can sensitively detect PGE<sub>2</sub> and 8-HOA levels in healthy and cancerous lung cells (BEAS2B and A549 respectively) in order to validate the effectivity of this new strategy in lung cancer treatment as well as in-time guidance during the therapy.

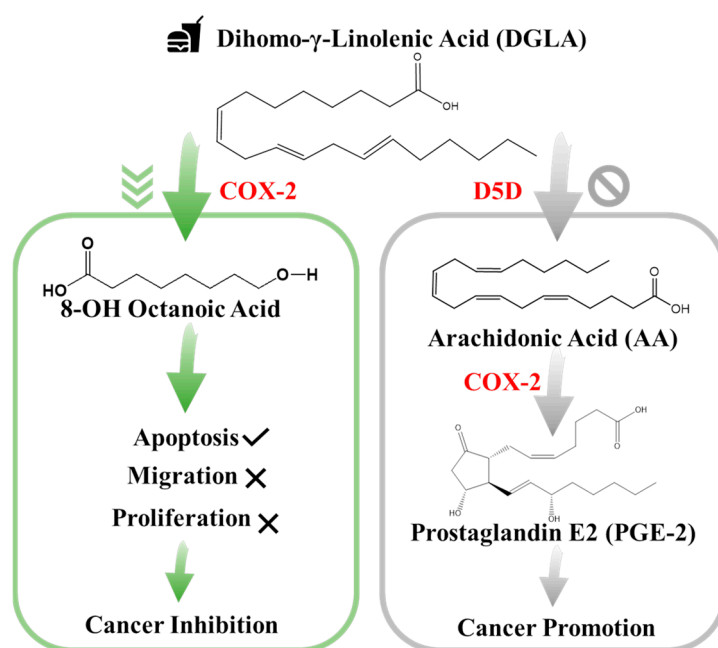
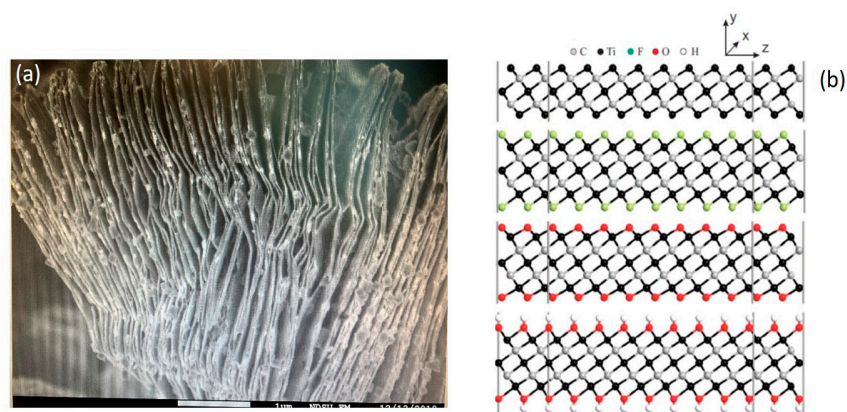


Figure 1. New anti-cancer strategy: target but not inhibit COX-2 in cancer.



**Figure 2.** Newly synthesized 2D multi-layered  $\text{Ti}_3\text{C}_2$  MXene nanosheets (a) Scanning Electron Microscope (SEM) image; (b) Pristine and surface-terminated  $\text{Ti}_3\text{C}_2$  MXene with different functional groups.

## 2. Materials and Methods

### 2.1. Sensing Material Synthesis and Cell Lines Preparation

#### 2.1.1. $\text{Ti}_3\text{C}_2$ Nanomaterial-Based Sensor Preparation

The sensor that we used is based on a new 2-D nanomaterial,  $\text{Ti}_3\text{C}_2$  MXene. This nanomaterial was prepared using a method developed in our group, named as the 'hot etching method' [47,48]. In details, the synthesis of  $\text{Ti}_3\text{C}_2$  MXene followed the steps: (1) Preparing  $\text{Ti}_3\text{AlC}_2$  MAX phase. It was obtained through ball milling TiC, Ti, Al powders in the molar ratio 2:1:1.2 for 5 h. Under argon flow, the resulting powder was then pressed into a pellet and sintered at 1350 °C for 4 h. The collected pellet after being milled back into powder was sieved through a 160-mesh sieve; (2) Etching Al from MAX phase to form MXene phase. The as-prepared MAX powder was collected at an elevated temperature for etching through 'hot-etch method'. HF acid in 25 mL Teflon line autoclave at a temperature of 150 °C was used in a Thermolyne furnace for 5 h to etch 0.5 g of MAX phase. To remove Al from MAX phase, 5 % wt of HF were used. Materials after being sonicated for one hour using a sonicating bath were collected through centrifuge; all the materials were dried overnight in a drying oven at 65 °C. (3) Synthesizing MXene powders for the sensing film. Finally, the synthesized nanomaterial was drop-casted on the gold electrode patterned glass substrate to form a thin film. The morphology of the synthesized 2D multilayered nanomaterial is shown in Figure 2a as the scanning electron microscope (SEM) image, which clearly exhibits multilayered nanosheets and accordion-like morphology. Figure 2b reveals the as-synthesized  $\text{Ti}_3\text{C}_2$  material's special surface terminations, which can lead to unique surface and material properties of  $\text{Ti}_3\text{C}_2$ .

#### 2.1.2. Cancer Cell Lines and Materials

A549 (ATCC®CCL-185™), and BEAS-2B (ATCC®CRL-9609™) were purchased from American Type Culture Collection (ATCC, VA, USA). Iminodibenzyl (CAS Number: 494-19-9) and 8-hydroxyoctanoic acid (8-HOA) were obtained from Sigma-Aldrich (St. Louis, MO, USA). PGE<sub>2</sub> and DGLA (for in vitro study), DGLA ethyl ester (for in vivo study), were acquired from Cayman Chemical (MI, USA).

#### 2.1.3. Preparation of Cell Samples

About  $3 \times 10^5$  A549 or BEAS-2B cells were trypsinized and seeded into each well of the 6-well plates. Then the cells were randomly assigned into different groups for the administration of DGLA (100 μM), iminodibenzyl (10 μM), or their combination accordingly. After 48 hours, the cell culture medium was collected. Cells were washed with PBS and collected by centrifugation after

trypsinization. A 1 mL cell culture medium with collected cells was homogenate and ready for testing. Three different groups of control samples were prepared using the same preparation procedures, including (a) blank group in 1 mL cell homogenate without any treatment; (b) 8-HOA group in 1 mL cell homogenate containing 0.6 ug/mL exogenous 8-HOA; (c) PGE<sub>2</sub> group in 1 mL cell homogenate containing 6 ug/mL exogenous PGE<sub>2</sub>.

#### 2.1.4. Xenografted Lung Tumor Model on Nude Mice

Six-week-old nude mice (nu/nu) mice were purchased from The Jackson Laboratory. The mice were housed in a pathogen-free IVC System with water and food ad libitum. All the animal experiments in this study were approved by the Institutional Animal Care and Use Committees at North Dakota State University. About  $2 \times 10^6$  A549 cells were injected into the hind flank of the nude mouse to induce tumors as we previously described [26]. The mice were randomly assigned to the following treatments: Control (treated with the same volume of the vehicle), DGLA (5 mg/mouse, oral gavage, every day), iminodibenzyl (15 mg/kg, intraperitoneal injection, every day) and DGLA+ iminodibenzyl. The treatment was started at two weeks of injection of A549 cells in nude mice. All the administrations lasted for four weeks. At end of the treatment, mice were sacrificed and tumors were isolated. Tumor tissues were crushed and homogenized by using a mortar in liquid nitrogen. The blood was centrifuged for 10 min at 2000 rpm for separating serum. The supernatant of tumor tissues and serum was collected for analysis.

#### 2.2. Methodology

To verify the roles of 8-HOA and PGE<sub>2</sub> in cancer development and treatment, the experiments have been designed to do testing in healthy lung cells and A549 lung cancer cells.

##### Normal cells

For application to test the effect of 8-HOA and PGE<sub>2</sub> in normal lung cells,  $10^6$  BEAS2B non-tumorigenic epithelial cell lines were collected. 8-HOA, PGE<sub>2</sub> and BSA (Bovine Serum Albumin) were applied to the samples right before measuring the resistance change. Once the samples were applied onto the Ti<sub>3</sub>C<sub>2</sub>MXene-based sensors, resistances were measured immediately and repeated at regular time intervals. The experiment is listed in the Table 1 and the resistance change of the MXene slides for each of the samples is measured and shown in Figure 3. The resistance increases dramatically when BEAS2B with PGE<sub>2</sub> is added but BEAS2B alone and BEAS2B with 8-HOA does not show obvious change of resistance.

**Table 1.** Table showing the composition of each sample for BEAS2B.

Sample	Cell	8-HOA	PGE <sub>2</sub>	BSA
1	$10^6$ BEAS2B	none	none	None
2	$10^6$ BEAS2B	0.6 ug/mL	none	None
3	$10^6$ BEAS2B	none	6 ug/mL	None
4	None	none	none	1 mg/mL

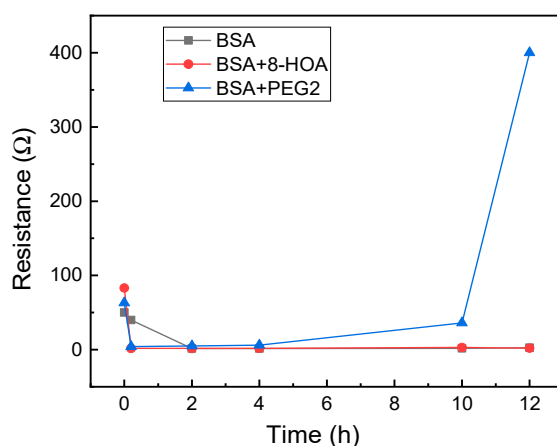


**Figure 3.** Resistance change measured using  $Ti_3C_2$  MXene-based sensors for BEAS2B cells.

### A549 lung cancer cells

A549 lung cancer epithelial cell lines were collected after being cultured. Similar to the BEAS-2B cell lines, 8-HOA and  $PGE_2$  samples were applied to the A549 cell lines just before conducting the experiment. The complete design of the experiments to verify the relative concentration of generated 8-HOA and  $PGE_2$  with and without using the new cancer treatment are listed in the Table 2.

**Table 2.** The composition of each sample for A549 cells treated by 8-hydroxyoctanoic acid (8-HOA), Prostaglandin  $E_2$  ( $PGE_2$ ), dihomo- $\gamma$ -linolenic acid (DGLA), delta-5-desaturase (D5Di) and DGLA + D5Di.

Sample	Cell	DGLA	D5Di	8-HOA	$PGE_2$	Estimated 8-HOA/ $PGE_2$ Level
1	$10^6$ A549	none	none	none	none	Low 8-HOA; low $PGE_2$
2	$10^6$ A549	none	none	0.6 ug/mL	none	High 8-HOA; low $PGE_2$
3	$10^6$ A549	none	none	none	6 ug/mL	Low 8-HOA; high $PGE_2$
4	$10^6$ A549	100 uM	none	none	none	Low 8-HOA; high $PGE_2$
5	$10^6$ A549	none	10 uM	none	none	Low 8-HOA; low $PGE_2$
6	$10^6$ A549	100 uM	10 uM	none	none	High 8-HOA; low $PGE_2$

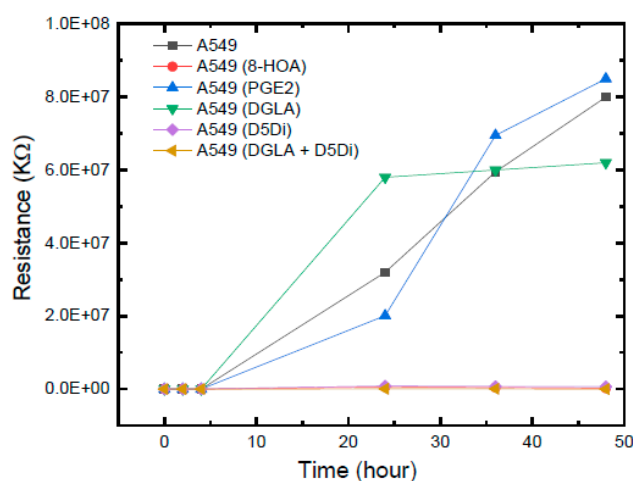


**Figure 4.** Resistance change measured using  $Ti_3C_2$  MXene-based sensors for A549 cancer cells with and without using the new anti-cancer treatment.



The sensing tests of these samples are shown in Figure 4. The resistances of A549 cancer cells, A549 cells treated by DGLA, and PGE<sub>2</sub> are much higher than the cancer cells treated by adding 8-HOA, applying D5Di, or using the new anti-cancer treatment DGLA + D5Di.

### 3. Results and Discussion

#### 3.1. Observation from the Non-Tumorigenic Sample Graph

In a healthy subject, both the concentration of PGE<sub>2</sub> and 8-HOA should be low. The sensing test is conducted on the normal lung cell, BEAS2B without extra treatment and BEAS2B by treating with extra PGE<sub>2</sub> or 8-HOA. Significant resistance increase is observed in BEAS2B by adding 10 μM PGE<sub>2</sub> while the untreated normal cells and cells treated by 8-HOA do not show obvious resistance change. This result indicates a unique role of PGE<sub>2</sub> in cells through the change of electrical property of cells. Considering the elevated concentration of PGE<sub>2</sub> can indicate a cancer development, such a sensitive response to PGE<sub>2</sub> using Ti<sub>3</sub>C<sub>2</sub>MXene-based sensor can be potentially used to diagnose cancer even at a very early stage.

#### 3.2. Observation from the CARCINOGENIC Samples (1st Trial)

As we have discussed in this paper previously, D5D inhibitor (D5Di) is used for preventing the conversion of DGLA to AA and ultimately limiting the formation of PGE<sub>2</sub>. According to the main mechanism of the new anti-cancer strategy, D5Di along with DGLA can effectively limit the formation of PGE<sub>2</sub> but promote the formation of 8-HOA. The sensing test using the newly developed Ti<sub>3</sub>C<sub>2</sub>MXene-based sensor, as shown in Figure 4, exhibits an interesting trend of resistance change. Similar to showing high resistance for A549, A549 with adding 10 μM PGE<sub>2</sub>, and A549 treated by DGLA both show high resistance as well. The results indicate a higher concentration of PGE<sub>2</sub> generated in A549 cells just by using DGLA, which confirms that omega-6 (DGLA) are pro-inflammatory and promote the formation of PGE<sub>2</sub>. However, the new anti-cancer treatment using DGLA and D5Di to treat A549 cells shows the similar resistance level as that of A549 cells with 8-HOA. This result provides promising information: the Ti<sub>3</sub>C<sub>2</sub>MXene-based sensor can be used to monitor or validate the anti-cancer effect of the new strategy: DGLA + D5Di, which should be an effective anti-cancer effect due to the generation of 8-HOA. This result is consistent with the results using GC-MS to confirm the new anti-cancer effect, as shown in Figure 5 [49].

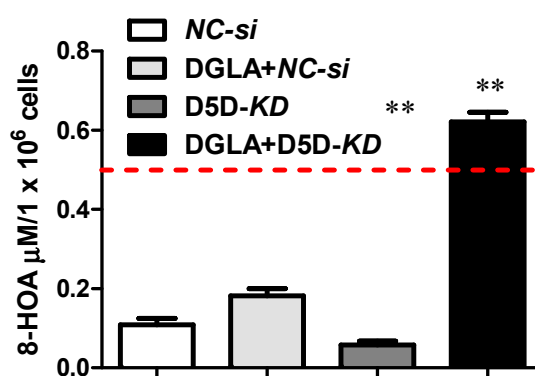


Figure 5. Effect of DGLA and D5D siRNA on 8-HOA formation.

### 4. Conclusions and Discussion

The preliminary results lead to an important conclusion: the Ti<sub>3</sub>C<sub>2</sub>-based sensor can be used as a convenient and simple method tool for anti-cancer treatment guidance and monitoring to sensitively detect the trace concentrations of PGE<sub>2</sub> and 8-HOA. Instead of using heavy, expensive and time-consuming GC-MS to assist the anti-cancer treatment, Ti<sub>3</sub>C<sub>2</sub>MXene based sensor can provide a faster, easier, efficient and much less invasive assistant tool to detect and cure cancer.

## References

1. Cancer. Available online: <https://www.who.int/news-room/fact-sheets/detail/cancer> (accessed on 10 October 2020).
2. Small Cell Lung Cancer—Cancer Therapy Advisor. Available online: <https://www.cancertherapyadvisor.com/home/decision-support-in-medicine/imaging/small-cell-lung-cancer/> (accessed on 10 October 2020).
3. Molina, J.R.; Yang, P.; Cassivi, S.D.; Schild, S.E.; Adjei, A.A. Non-small cell lung cancer: Epidemiology, risk factors, treatment, and survivorship. *Mayo Clin. Proc.* **2008**, *83*, 584–594.
4. LTorre, A.; Siegel, R.L.; Jemal, A. Lung cancer statistics. *Adv. Exp. Med. Biol.* **2016**, *893*, 1–19.
5. Asbestos Lung Cancer: Causes, Diagnosis & Treatment. Available online: <https://www.asbestos.com/cancer/lung-cancer/> (accessed on 10 October 2020).
6. Deadliest Cancers Receive the Least Attention. Available online: <https://www.asbestos.com/featured-stories/cancers-that-kill-us/> (accessed on 11 October 2020).
7. Cruz, C.S.D.; Tanoue, L.T.; Matthay, R.A. Lung Cancer: Epidemiology, Etiology, and Prevention. *CME* **2011**, *32*, 605–644.
8. Lee, S.H. Chemotherapy for lung cancer in the era of personalized medicine. *Tuberc. Respir. Dis. (Seoul)* **2019**, *82*, 179–189.
9. Cheng, M.; Jolly, S.; Quarshie, W.O.; Kapadia, N.; Vigneau, F.D.; Kong, F.M. Modern radiation further improves survival in non-small cell lung cancer: An analysis of 288,670 patients. *J. Cancer* **2019**, *10*, 168–177.
10. Sandler, A.B.; Dubinett, S.M. COX-2 inhibition and lung cancer. *Semin. Oncol.* **2004**, *31*, 7, 45–52.
11. Vega, O.M.; Abkenari, S.; Tong, Z.; Tedman, A.; Huerta-Yepez, S. Omega-3 Polyunsaturated Fatty Acids and Lung Cancer: nutrition or Pharmacology? *Nutr. Cancer* **2020**, 1–21.
12. Yin, Y.; Sui, C.; Meng, F.; Ma, P.; Jiang, Y. The omega-3 polyunsaturated fatty acid docosahexaenoic acid inhibits proliferation and progression of non-small cell lung cancer cells through the reactive oxygen species-mediated inactivation of the PI3K /Akt pathway. *Lipids Health Dis.* **2017**, *16*, 87.
13. Kouremenos, K.A.; Johansson, M.; Marriott, P.J. Advances in gas chromatographic methods for the identification of biomarkers in cancer. *J. Cancer* **2012**, *3*, 404–420.
14. Cancer—Diagnosis and Treatment—Mayo Clinic. Available online: <https://www.mayoclinic.org/diseases-conditions/cancer/diagnosis-treatment/drc-20370594> (accessed on 10 October 2020).
15. Problems with MRI for Cancer Diagnosis. Available online: <https://www.ctoam.com/precision-oncology/why-we-exist/standard-treatment/diagnostics/mri/> (accessed on 12 October 2020).
16. The Pros and Cons of PET/CT Scans | Independent Imaging. Available online: <https://www.independentimaging.com/the-pros-and-cons-of-pet-ct-scans/> (accessed on 12 October 2020).
17. Fred, H.L. Drawbacks and limitations of computed tomography: Views from a medical educator. *Tex. Heart Inst. J.* **2004**, *31*, 345–348.
18. Bitencourt, A.G.V.; Graziano, L.; Guatelli, C.S.; Albuquerque, M.L.L.; Marques, E.F. Ultrasound-guided biopsy of breast calcifications using a new image processing technique: Initial experience. *Radiol. Bras.* **2018**, *51*, 106–108.
19. Endoscopy: Purpose, Procedure, Risks. Available online: <https://www.webmd.com/digestive-disorders/digestive-diseases-endoscopy#1> (accessed on 13 October 2020).
20. Gas Chromatography. Available online: [http://www.chemforlife.org/teacher/topics/gas\\_chromatography.htm](http://www.chemforlife.org/teacher/topics/gas_chromatography.htm) (accessed on 13 October 2020).
21. Buszewski, B.; Ligor, T.; Jezierski, T.; Wenda-Piesik, A.; Walczak, M.; Rudnicka, J. Identification of volatile lung cancer markers by gas chromatography-mass spectrometry: Comparison with discrimination by canines. *Anal. Bioanal. Chem.* **2012**, *404*, 141–146.
22. Borer, J.S.; Simon, L.S. Cardiovascular and gastrointestinal effects of COX-2 inhibitors and NSAIDs: Achieving a balance. *Arthritis Res. Ther.* **2005**, *7*, S14.
23. Yang, P.; Chan, D.; Felix, E.; Cartwright, C. Formation and antiproliferative effect of prostaglandin E3 from eicosapentaenoic acid in human lung cancer cells. *J. Lipid Res.* **2004**, *45*, 1030–1039.
24. Xu, Y.; Qi, J.; Yang, X.; Wu, E.; Qian, S.Y. Free radical derivatives formed from cyclooxygenase-catalyzed dihomogamma-linolenic acid peroxidation can attenuate colon cancer cell growth and enhance 5-fluorouracil's cytotoxicity. *Redox Biol.* **2014**, *2*, 610–618.



25. Xu, Y.; Yang, X.; Wang, T.; Yang, L.; He, Yu.; Miskimins, K.; Qian, S.Y. Knockdown delta-5-desaturase in breast cancer cells that overexpress COX-2 results in inhibition of growth, migration and invasion via a dihomo- $\gamma$ -linolenic acid peroxidation dependent mechanism. *BMC Cancer* **2018**, *18*, 1–15.
26. Pang, L.; Shah, H.; Wang, H.; Shu, D.; Qian, S.Y.; Sathish, V. EpCAM-Targeted 3WJ RNA Nanoparticle Harboring Delta-5-Desaturase siRNA Inhibited Lung Tumor Formation via DGLA Peroxidation. *Mol. Ther. Nucleic Acids* **2020**, *22*, 222–235.
27. Yang, X.; Xu, Y.; Wang, T.; Shu, D.; Guo, P.; Miskimins, K.; Qian, S.Y. Inhibition of cancer migration and invasion by knocking down delta-5-desaturase in COX-2 overexpressed cancer cells. *Redox Biol.* **2017**, *11*, 653–662.
28. Jafarizadeh-Malmiri, H.; Sayyar, Z.; Anarjan, N.; Berenjian, A. Nano-sensors in Food Nanobiotechnology. In *Nanobiotechnology in Food: Concepts, Applications and Perspectives*; Springer International Publishing: Basel, Switzerland, 2019, pp. 81–94.
29. Wang, P.; Zhang, L.; Zheng, W.; Cong, L.; Guo, Z.; Xie, Y.; Wang, L.; Tang, R.; Feng, Q.; Hamada, Y.; et al. Thermo-triggered Release of CRISPR-Cas9 System by Lipid-Encapsulated Gold Nanoparticles for Tumor Therapy. *Angew. Chem. Int. Ed.* **2018**, *57*, 1491–1496.
30. Lei, Y.; Tang, L.; Xie, Y.; Xianyu, Y.; Zhang, L.; Wang, P.; Hamada, Y.; Jiang, K.; Zheng, W.; Jiang, X. Gold nanoclusters-assisted delivery of NGF siRNA for effective treatment of pancreatic cancer. *Nat. Commun.* **2017**, *8*, 1–15.
31. Li, N.; Wu, D.; Li, X.; Zhou, X.; Fan, G.; Li, G.; Wu, Y. Effective enrichment and detection of plant growth regulators in fruits and vegetables using a novel magnetic covalent organic framework material as the adsorbents. *Food Chem.* **2020**, *306*, 125455.
32. Wang, D.; Zhang, Q.; Hossain, M.R.; Johnson, M. High Sensitive Breath Sensor Based on Nanostructured K2W7O22 for Detection of Type 1 Diabetes. *IEEE Sens. J.* **2018**, *18*, 4399–4404.
33. Huber, F.; Riegert, S.; Madel, M.; Thonke, K. H2S sensing in the ppb regime with zinc oxide nanowires. *Sens. Actuatorsb Chem.* **2017**, *239*, 358–363.
34. Wang, C.; Chu, X.; Wu, M. Detection of H2S down to ppb levels at room temperature using sensors based on ZnO nanorods. *Sens. Actuatorsb Chem.* **2006**, *113*, 320–323.
35. Rai, P.; Majhi, S.M.; Yu, Y.T.; Lee, J.H. Noble metal@metal oxide semiconductor core@shell nano-architectures as a new platform for gas sensor applications. *Rsc Adv.* **2015**, *5*, 76229–76248.
36. Korotcenkov, G.; Brinzari, V.; Cho, B.K. Conductometric gas sensors based on metal oxides modified with gold nanoparticles: a review. *Microchim. Acta* **2016**, *183*, 1033–1054.
37. Wang, D.L.; Chen, A.T.; Zhang, Q.F.; Cao, G.Z. Room-Temperature Chemiresistive Effect of TiO<sub>2</sub>–B Nanowires to Nitroaromatic and Nitroamine Explosives. *IEEE Sens. J.* **2011**, *11*, 1352–1358.
38. Wang, D.; Sun, H.; Chen, A.; Jang, S.H.; Jen, A.K.Y.; Szep, A. Chemiresistive response of silicon nanowires to trace vapor of nitro explosives. *Nanoscale* **2012**, *4*, 2628–2632.
39. Wang, T.; Huang, D.; Yang, Z.; Xu, S.; He, G.; Li, X.; Hu, N.; Yin, G.; He, D.; Zhang, L. A Review on Graphene-Based Gas/Vapor Sensors with Unique Properties and Potential Applications. *Nano-Micro Lett.* **2016**, *8*, 95–119.
40. Toda, K.; Furue, R.; Hayami, S. Recent progress in applications of graphene oxide for gas sensing: A review. *Anal. Chim. Acta* **2015**, *878*, 43–53.
41. Ji, J.; Wen, J.; Shen, Y.; Lv, Y.; Chen, Y.; Liu, S.; Ma, H.; Zhang, Y. Simultaneous Noncovalent Modification and Exfoliation of 2D Carbon Nitride for Enhanced Electrochemiluminescent Biosensing. *J. Am. Chem. Soc.* **2017**, *139*, 11698–11701.
42. Tan, C.; Cao, X.; Wu, X.; He, Q.; Recent Advances in Ultrathin Two-Dimensional Nanomaterials. *Chem. Rev.* **2017**, *117*, 6225–6331.
43. Wen, W.; Song, Y.; Yan, X.; Zhu, C.; Du, D.; Wang, S.; Asiri, A.; Lin, Y. Recent advances in emerging 2D nanomaterials for biosensing and bioimaging applications. *Mater. Today* **2018**, *21*, 164–177.
44. Ghidui, M.; Lukatskaya, M.R.; Zhao, M.Q.; Gogotsi, Y.; Barsoum, M.W. Conductive two-dimensional titanium carbide ‘clay’ with high volumetric capacitance. *Nature* **2015**, *516*, 78–81.
45. Peng, Q.; Guo, J.; Zhang, Q.; Xiang, J.; Liu, B.; Zhou, A.; Liu, R.; Tian, Y. Unique lead adsorption behavior of activated hydroxyl group in two-dimensional titanium carbide. *J. Am. Chem. Soc.* **2014**, *136*, 4113–4116.
46. Kim, S.J.; Koh, H.; Ren, C.E.; Kwon, O.; Maleski, K.; Cho, S.; Anasori, B.; Kim, C.; Choi, Y.; Kim, J.; et al. Metallic Ti<sub>3</sub>C<sub>2</sub>T<sub>x</sub> MXene Gas Sensors with Ultrahigh Signal-to-Noise Ratio. *ACS Nano* **2018**, *12*, 986–993.

47. Michael, J.; Qifeng, Z.; Danling, W. Titanium carbide MXene: Synthesis, electrical and optical properties and their applications in sensors and energy storage devices. *Nanomater. Nanotechnol.* **2019**, *9*, 184798041882447.
48. Alhabeab, M.; Maleski, K.; Anasori, B.; Lelyukh, P.; Clark, L.; Sin, S.; Gogotsi, Y. Guidelines for Synthesis and Processing of Two-Dimensional Titanium Carbide ( $Ti_3C_2T_x$  MXene). *Chem. Mater.* **2017**, *29*, 7633–7644.
49. Pang, L.; Shah, H.; Zhao, P.; Qian, S.; Sathish, V. New Delta-5-Desaturase Inhibitor Suppress Lung Cancer Progression: A Paradigm Shift on COX-2 Biology in Lung Cancer Treatment. *FASEB J.* **2020**, *34*, 1.

**Publisher's Note:** MDPI stays neutral with regard to jurisdictional claims in published maps and institutional affiliations.



© 2020 by the authors. Licensee MDPI, Basel, Switzerland. This article is an open access article distributed under the terms and conditions of the Creative Commons Attribution (CC BY) license (<http://creativecommons.org/licenses/by/4.0/>).